Appl Phys A (2010) 101: 503–508
DOI 10.1007/s00339-010-5887-6

Applied Physics A
Materials Science & Processing

Super-hydrophobic transparent surface by femtosecond laser micro-patterned catalyst thin film for carbon nanotube cluster growth

M. Tang · M.H. Hong · Y.S. Choo · Z. Tang · Daniel H.C. Chua

Received: 18 November 2009 / Accepted: 24 May 2010 / Published online: 2 July 2010

Abstract In this work, super-hydrophobic surfaces were fabricated by femtosecond laser micro-machining and chemical vapor deposition to constitute hybrid scale micro/nano-structures formed by carbon nanotube (CNT) clusters. Nickel thin-film microstructures, functioning as CNT growth catalyst, precisely control the distribution of the CNT clusters. To obtain minimal heat-affected zones, femtosecond laser was used to trim the nickel thin-film coating. Plasma treatment was subsequently carried out to enhance the lotus-leaf effect. The wetting property of the CNT surface is improved from hydrophilicity to super-hydrophobicity at an advancing contact angle of 161 degrees. The dynamic water drop impacting test further confirms its enhanced water-repellent property. Meanwhile, this super-hydrophobic surface exhibits excellent transparency with quartz as the substrate. This hybrid fabrication technique can achieve super-hydrophobic surfaces over a large area, which has potential applications as self-cleaning windows for vehicles, solar cells and high-rise buildings.

M. Tang · M.H. Hong (✉)
Department of Electrical and Computer Engineering, National University of Singapore, 117576, Singapore, Republic of Singapore
e-mail: elehmh@nus.edu.sg

M. Tang · Y.S. Choo
Department of Civil Engineering, National University of Singapore, Singapore, 117576, Republic of Singapore

Z. Tang · D.H.C. Chua
Department of Materials Science and Engineering, National University of Singapore, Singapore, 117574, Republic of Singapore

1 Introduction

Artificial super-hydrophobic surfaces are potentially suitable for applications in dust-free and self-cleaning surfaces [1]. The transparent super-hydrophobic surface is capable of preventing the contamination of a transparent substrate. It can be widely applied as self-cleaning windows of vehicles, solar cells and high-rise buildings. In nature, various super-hydrophobic surfaces, like lotus leaf and rice leaf, which have small and fractal structures on their surfaces, have been found with water contact angles greater than 150° [2]. Taking the advantage of small contact areas with water, chemical reactions or bond formations between water and the super-hydrophobic surfaces would be limited. To fabricate super-hydrophobic surfaces, surface wettability is an important characteristic feature of functional materials, which is governed both by their surface energy and surface roughness [3]. Material surfaces with a low surface energy are usually water repellent. The surface roughness can be further enhanced and associated with wetting properties [4]. Therefore, various fractal micro/nano-structures, for example nanopins, nanorods, nanofibers, nanofilaments, colloidal microstructures, honeycomb-like membranes and inorganic fractals, have been introduced to make super-hydrophobic surfaces [5, 6].

In recent researches for transparent super-hydrophobic surfaces, the surface roughness is controlled within the range of one hundred nanometers. Kim et al. have fabricated a super-hydrophobic and highly transparent nano-structured film via imprinting and conformally uniform chemical anchoring of poly (dimethylsiloxane) [7]. Ling et al. have created a super-hydrophobic surface by "dip-coating" of 60-nm SiO_2 nanoparticles onto an amine-terminated (NH_2) self-assembled monolayer (SAM) glass/silicon oxide substrate, followed by chemical vapor deposition (CVD) of

a fluorinated adsorbate [8]. The contact angles of super-hydrophobic surfaces in these research works were less than 160°. Some research groups worked on super-hydrophobic surfaces by carbon nanotube (CNT) coating. Lao et al. have made a super-hydrophobic surface of CNTs through vertically aligned CNTs at a water contact angle of 168° by modifying the surface of vertically aligned nanotubes with a hydrophobic poly-tetra fluoroethylene (PTFE) coating [9]. Li et al. have synthesized super-hydrophobic bionic surfaces with hierarchical micro/nano-structures by decorating CNTs on monolayer polystyrene colloidal crystals with a wet chemical self-assembly technique to achieve a water contact angle of 166° [10]. Although the CNT coated surface is a promising candidate to fabricate a super-hydrophobic surface, the CNTs inevitably increase the surface roughness, which results in a non-transparent surface [11]. In order to achieve a super-hydrophobic surface with high transparency, patterned CNT clusters over a large area by femtosecond laser micro-machining and CVD are demonstrated in this paper.

2 Experimental details

The processing diagram to fabricate square-shaped CNT clusters is shown in Fig. 1. The process flow can be summarized in four steps. Firstly, a nickel thin film with the thickness of ∼10 nm was coated on the quartz surface by an electron-beam evaporator. This was used as a catalyst to control the CNT growth. The thickness of nickel thin film affects the density and size of the CNTs. Secondly, femtosecond laser micro-machining was used to pattern the nickel thin film. The key component is Ultrafast Ti: Sapphire laser (Tsunami Model 3960) with a regenerative amplifier (Spitfire Model F-1K) from Spectra physics. The wavelength is 800 nm and the pulse duration is 100 fs. The pulse repetition rate was fixed at 1 kHz, and the maximum pulse energy is up to 1 mJ. The system is also equipped with a beam attenuator in order to tune the output power. The laser beam was focused into a spot with the size of a few micrometers in diameter by a Mitutoyo M-plan NIR 50× objective lens. Three-axis motorized stage was placed beneath the objective lens. The quartz substrate coated with the nickel thin film was fixed on the stage. The laser beam irradiated the nickel thin film perpendicularly. The stage along the optical axis can shift the nickel thin film to the laser focus plane guided by a CCD camera. By controlling the sample stage movement within the two horizontal axes, the well-focused laser beam is able to trim the nickel film from the quartz substrate [12]. Compared to conventional photolithography, the femtosecond laser micro-machining is a maskless process [13]. Arbitrary patterns could be flexibly fabricated through modifying the computer-controlled graphic

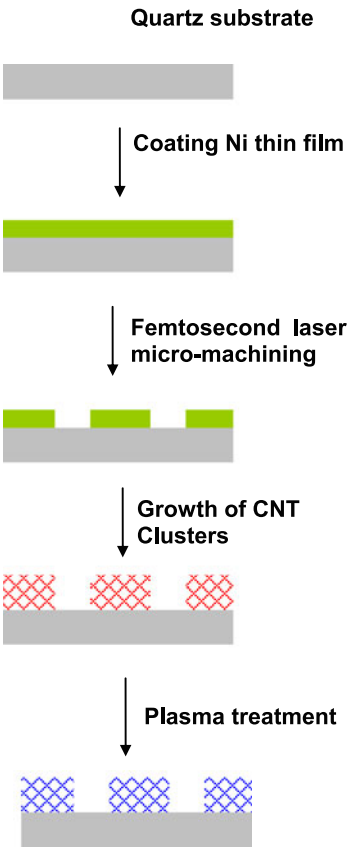

Fig. 1 Processing flow of super-hydrophobic surface fabrication by femtosecond laser micro-machining and chemical vapor deposition

software. Thirdly, CNTs were grown inside a CVD chamber on the quartz substrate with patterned nickel thin film. The chamber was charged with acetylene gas. Carbon nanotubes were grown at a temperature of 650°C for 10 min. The last step was plasma treatment of the CNT clusters in a reactive ion etching (RIE) system. The plasma treatment was carried out by using CHF_3 gas at a flow rate of 55 sccm for 10 seconds [14]. The morphology of the CNT clusters grown on the quartz substrates was examined with field emission scanning electron microscopy (SEM, Hitachi S4100) with energy-dispersive X-ray spectroscopy (EDX). Water contact angle measurements were performed with a goniometer (AST Products Inc., VCA Optima-XE) and a high-speed camera (FastCam X1024) was used to capture the dynamic behavior of water droplet on the surface of patterned CNT clusters.

3 Results and discussion

Femtosecond laser micro-machining was applied to trim nickel thin film coated on the quartz substrate. The pulse duration of the femtosecond laser is very short so that there is insufficient time for the pulse energy to be distributed to

the substrate in the form of heat. Thus, particularly at low pulse energies, there is minimal or no heat-affected zone (HAZ) [15]. The depth of focus for the objective lens with 50× magnification is smaller than 5 μm. Hence, great attention is needed during searching for the laser focus plane with the assistance of the CCD camera. The laser fluence was set at 33 J/cm^2 and pulse repetition rate was 1 kHz. The scanning speed was 100 mm/min. The femtosecond laser micro-machining is able to fabricate the square micro-patterns at well-controlled size and pitch. The femtosecond laser can remove the nickel thin film cleanly without thermal effects to affect the surrounding or substrate layers. But the focused laser beam scratches the quartz surface slightly and forms shallow nano-grooves. The nickel nanoparticles, generated from plasma species in the laser micro-machining, scatter around the processed surface. Therefore, a few CNTs grow in the gaps of clusters.

After the laser micro-machining, the growth of CNT clusters was controlled by the nickel thin-film micro-patterns [16]. CVD was used to grow large-scale CNTs on the substrate coated with Ni catalyst. When the sample was heated up to 650°C, the initially continuous Ni thin film was broken into droplets (nanometers in size). These droplets are the necessary precursors for the catalytic growth of CNTs. After the acetylene was introduced into the chamber, the CNTs started to grow. The length of CNTs can be controlled by the growing time [17]. SEM images of the CNT clusters from micro-scale to nano-scale are illustrated in Fig. 2. The CNT clusters can be fabricated over a large area as shown in Fig. 2(a). The cluster size is 17 μm and the array pitch 30 μm, as shown in Fig. 2(b). The height of the CNT clusters is ∼5 μm, measured by a three-dimensional optical microscope (Microphase, Zeiss). Fibril-like morphology of CNT nanowires is shown in Fig. 2(c) at diameters ranging from 50 to 200 nm. The carbon nanotubes grow in a high density and most of them are twisted together [18].

The sample surface with CNT clusters is transparent. Figure 3(a) represents the image of the two characters "E" and "n" observed through the surface of CNT square clusters. At the visible wavelength range, CNT square clusters have transmittance up to 63%, which was measured by a UV-Vis spectroscope. The transmittance can be controlled by the size and pitch of the CNT clusters. Although CNT clusters are non-transparent, light can go through the gaps between adjacent clusters. Total transmittance of pattered CNT cluster surface can be estimated as:

$$T = \eta \cdot \frac{S_{\text{tot}} - S_{\text{CNT}}}{S_{\text{tot}}} = \eta \cdot \frac{b^2 - a^2}{b^2}, \tag{1}$$

where S_{tot} is the substrate area, S_{CNT} the area of the square CNT cluster and η the transmittance of uncovered area. The CNT square clusters are periodically arranged microstructures in two-dimensional planes, whereas a and b are

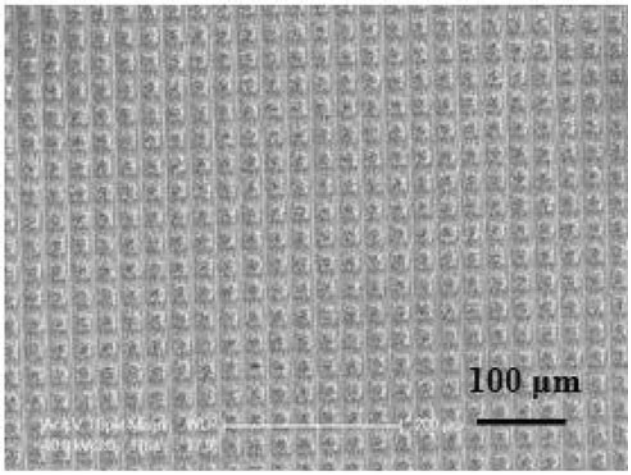

a

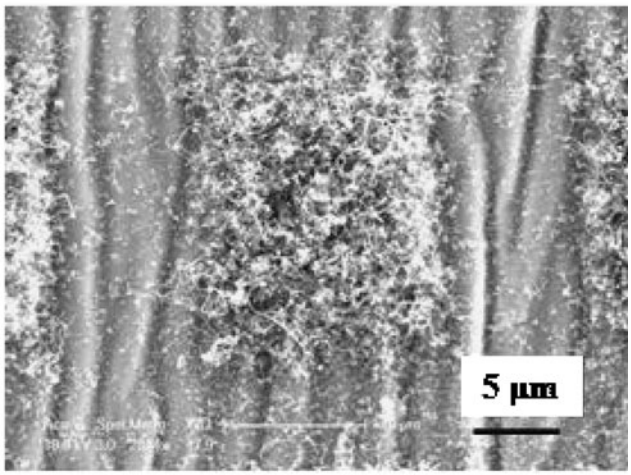

b

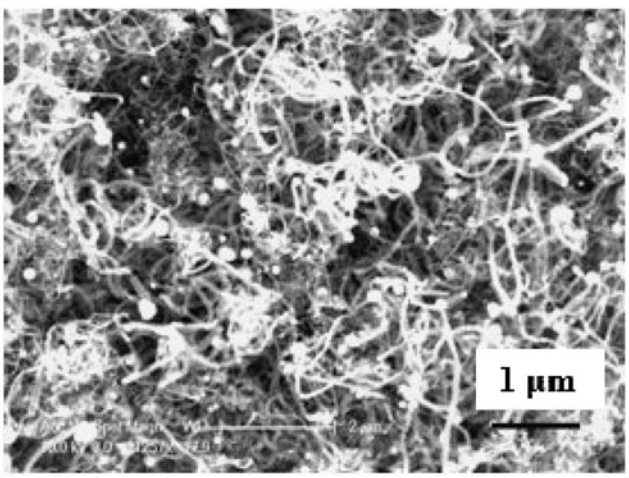

c

Fig. 2 Hybrid micro/nano-structures of CNT cluster super-hydrophobic surface made by femtosecond laser micro-machining and chemical vapor deposition

the size and pitch of the CNT square cluster, respectively as shown in Fig. 3(b). The areal ratio of the uncovered area over the substrate area is 69%. The measured transmit-

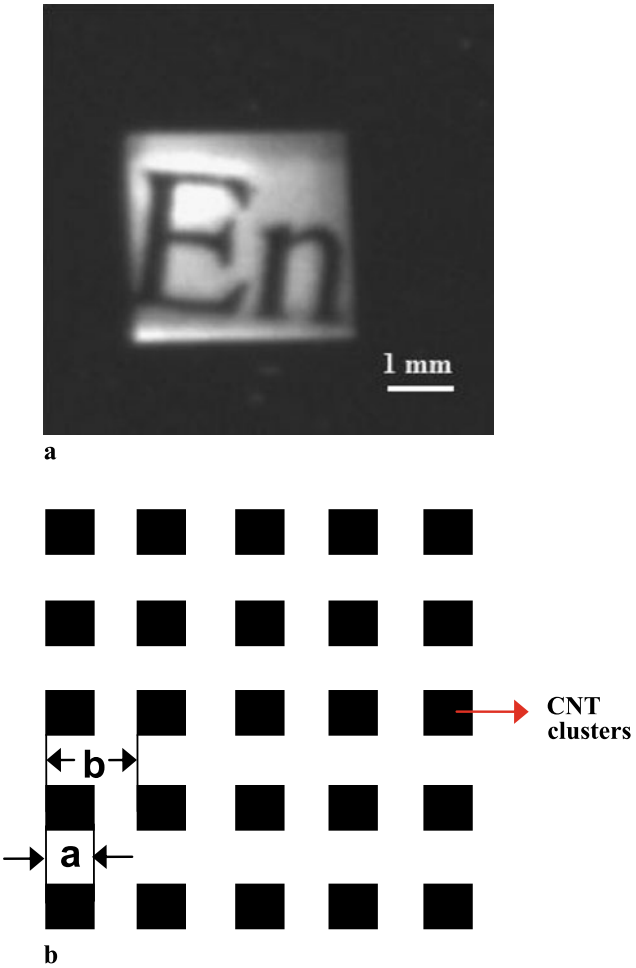

Fig. 3 (**a**) Optical microscope image and (**b**) schematic drawing of CNT cluster super-hydrophobic surface fabricated by femtosecond laser micro-machining and chemical vapor deposition

tance 63% is slightly lower. It is due to surface contaminations and nano-grooves existing in the gaps. The value of η, which represents the transmittance of the uncovered area, is 91% from the estimation. The image through the transparent super-hydrophobic surface becomes blurred at a long distance because the micro-pattern array diffracts optical light. Though surface roughness can enhance the hydrophobicity, surface roughness and transparency are competitive properties, which need to be comprised in the pattern design and fabrication. The patterned CNT clusters increase the roughness of quartz surface; however, the distribution of the surface roughness is not uniform [19]. Light can transmit through the CNT clusters uncovering region with low roughness. Due to the resolution of human eyes at ~100 μm, the whole CNT cluster region is visually uniform and transparent. Furthermore, this method is also different from the previous researches, in which super-hydrophobic surfaces were achieved by uniform roughness at tens of nanometers and transmitted light of those surfaces are dominated by Mie theory [20]. For our design, CNT clusters are much larger in size than the visible light wavelength and possess little diffractive effect.

Advancing contact angle of the water drops was measured with ultra-pure water. The advancing contact angle was measured by forming a drop on the surface and pumping liquid into it until its base expanded. After a few seconds for equilibration, the image of the water droplet was taken and the advancing contact angle was determined by using the graphic tools of image processing software [21]. The advancing contact angle is governed by the Cassie–Baxter equation as follows:

$$\cos\theta_{\mathrm{CB}} = f_{\mathrm{s}}(\cos\theta_1 + 1) - 1, \tag{2}$$

where θ_{CB} is the Cassie–Baxter contact angle, θ_1 the contact angle on smooth surface, and f_{s} the ratio of the rough surface area in contact with a water drop to the apparent surface area covered by the water drop [22]. It is clear that the top width of the groove should be as small as possible while maintaining a sufficiently large depth so as to reduce the parameter f_{s}. The surface of CNT clusters before the plasma treatment is hydrophilic or less hydrophobic. The advancing contact angle ranges from 80 to 130 degrees. This phenomenon is caused by the presence of hydrophilic functional group on the CNT surface. In the CNT growth process, the reaction chamber was pumped down to $\sim 10^{-5}$ bar. However, a small amount of oxygen and water molecules still remain inside the chamber. When CNT clusters stop growing but the chamber is still at a high temperature, oxygen and water molecules react with CNTs. The hydrophilic functional groups (e.g. –OH) can form on the surface of CNT clusters. CHF_3 plasma treatment in the RIE chamber was used to remove the hydrophilic layer from the CNTs. The process took ten seconds. Oxygen concentrations before and after the plasma treatment were examined by an EDX, as shown in Fig. 4. The concentration of oxygen atoms on the CNT surface can be significantly reduced after the plasma treatment. The substrate surface becomes super-hydrophobic as the advancing contact angle is increased up to 161 degree, as shown in Fig. 5.

To further study the super-hydrophobic property of the CNT clusters, the dynamic behavior of a water drop on the CNT clusters was also investigated. This was captured by a high-speed camera at a 1000 Hz frame rate and selected time sequence of images with the interval of 5 ms are presented in Fig. 6, which show the behavior of a droplet falling on the CNT cluster surface during its impact [23]. The impact velocity for this case was ~1 cm/s. As shown in the images, the droplet firstly deforms and flattens into a pancake shape, then retracts and finally rebounds off the surface. The droplet remains completely intact during the collision and does not splash or fragment into smaller droplets. The total contact time (~20 ms) of the droplet with the CNT cluster

surface was found to be independent of the impact velocity. The droplet advances and recedes at an angle greater than 90 degrees. The surface is super-hydrophobic so that the droplet has sufficient momentum to leave the surface. It can carry away the dust particles etc. deposited on the surface for the surface self-cleaning [24].

4 Conclusions

In summary, we report a flexible way to fabricate transparent super-hydrophobic surfaces. Nickel thin film was coated on the quartz surface by the electron-beam evaporation and then used as a catalyst to control the growth of carbon nanotubes. Femtosecond laser was applied to trim the nickel thin film on the quartz substrate and fabricate micro-square nickel patterns with minimal or no heat accumulation and dissipation. Carbon nanotubes were grown only on the areas covered by the nickel thin film by chemical vapor deposition. The carbon nanotubes forms square clusters in the well-controlled areas. To further enhance the lotus-leaf effect, plasma treatment was carried out and the wetting property of CNT cluster surface is improved from hydrophilicity to super-hydrophobicity with its advancing contact angle at 161 degrees. This super-hydrophobic film is still transpar-

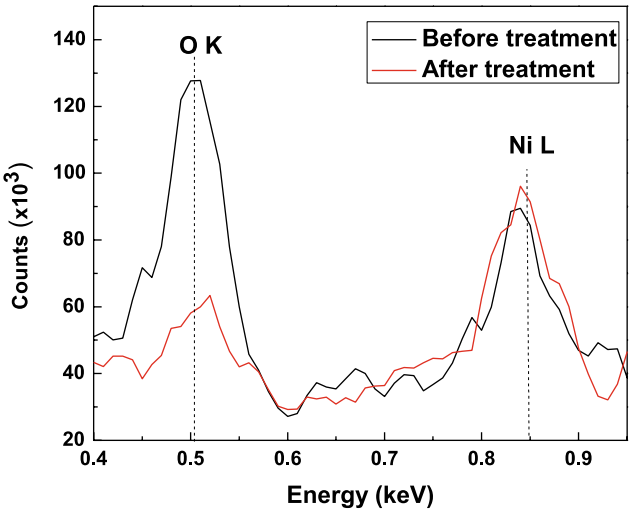

Fig. 4 EDX spectra of the CNT cluster surface before and after the plasma treatment

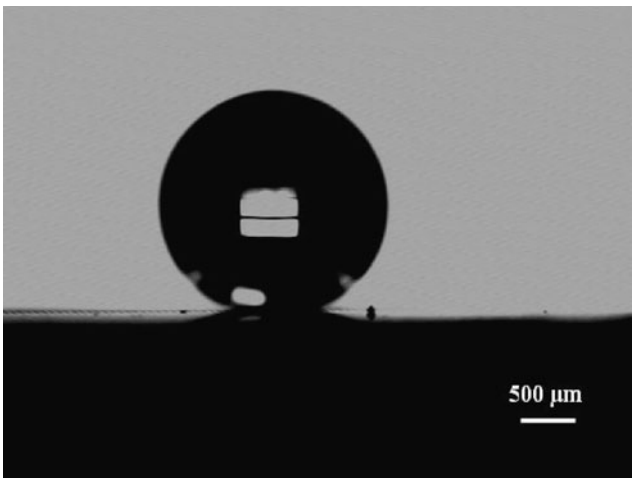

Fig. 5 Optical image of water droplet on the CNT cluster super-hydrophobic surface (advancing contact angle ~161 degrees)

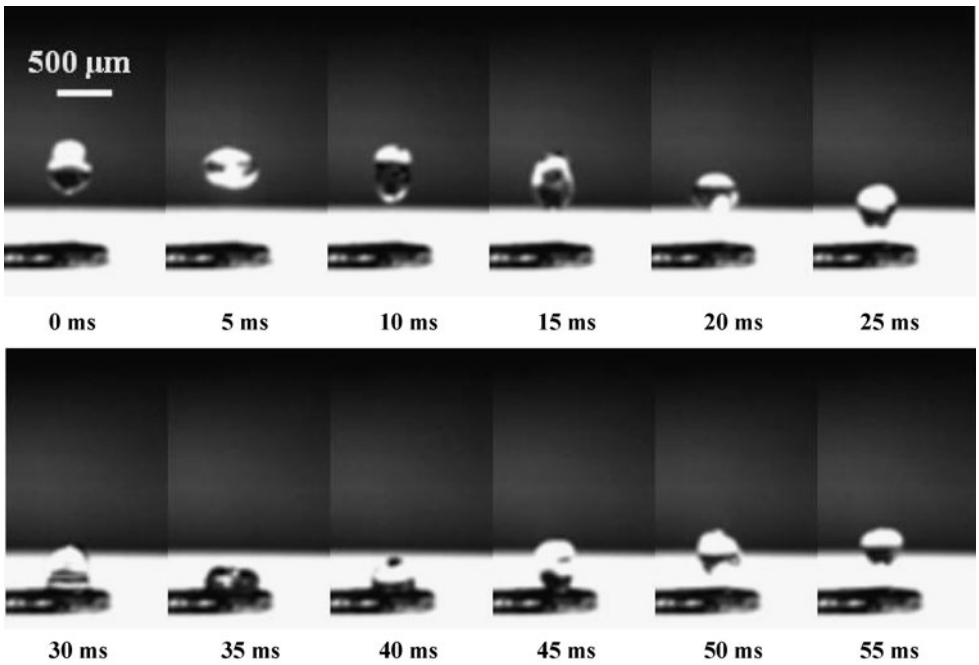

Fig. 6 Snapshots of a water droplet impacting on the super-hydrophobic surface of CNT cluster super-hydrophobic surface fabricated by femtosecond laser micro-machining and chemical vapor deposition

ent with 63% transmission. It can be further improved by controlling the size and pitch of patterned CNT clusters and scarifying some super-hydrophobicity property. The technique can be easily extended to a large area patterning by advanced laser micro-fabrication and CVD process. This simple and cost-effective method benefits the mass production of transparent and self-cleaning substrates as the windows for vehicles, solar cells and high-rise buildings.

Acknowledgements This work was funded by Lloyd's Register Professorship (WBS: R264002006720) in National University of Singapore.

References

1. L. Feng, S. Li, Y. Li, H. Li, L. Zhang, J. Zhai, Y. Song, B. Liu, L. Jiang, D. Zhu, Adv. Mater. **14**(24), 1857 (2002)
2. V. Zorba, E. Stratakis, M. Barberoglou, E. Spanakis, P. Tzanetakis, S.H. Anastasiadis, C. Fotakis, Adv. Mater. **20**, 4049 (2008)
3. C. Yang, U. Tartaglino, B.N.J. Persson, Phys. Rev. Lett. **97**(11), 116103 (2006)
4. L. Jiang, Y. Zhao, J. Zhai, Angew. Chem. Int. Ed. **43**(33), 4338 (2004)
5. E. Hosono, S. Fujihara, I. Honma, H. Zhou, J. Am. Chem. Soc. **127**(39), 13458 (2005)
6. M. Ma, R.M. Hill, Curr. Opin. Colloid Interface Sci. **11**(4), 193 (2006)
7. M. Kim, K. Kim, N.Y. Lee, K. Shin, Y.S. Kim, Chem. Commun. **2007**(22), 2237 (2007)
8. X.Y. Ling, I.Y. Phang, G.J. Vancso, J. Huskens, D.N. Reinhoudt, Langmuir **22**(7), 3081 (2009)
9. K.K.S. Lau, J. Bico, K.B.K. Teo, M. Chhowalla, G.A.J. Amaratunga, W.I. Milne, G.H. McKinley, K.K. Gleason, Nano Lett. **3**(12), 1701 (2003)
10. Y. Li, X.J. Huang, S.H. Heo, C.C. Li, Y.K. Choi, W.P. Cai, S.O. Cho, Langmuir **23**(4), 2169 (2007)
11. Z.J. Han, B.K. Tay, M. Shakerzadeh, K. Ostrikov, Appl. Phys. Lett. **94**, 223106 (2009)
12. M. Tang, M.H. Hong, Y.S. Choo, Paper presented at the Photonics-Global@Singapore, IPGC, IEEE, Singapore, 2008 (unpublished)
13. A. Pozzato, S.D. Zilio, G. Fois, D. Vendramin, G. Mistura, M. Belotti, Y. Chen, M. Natali, Microelectron. Eng. **83**(4–9), 884 (2006)
14. Y.C. Hong, D.H. Shin, S.C. Cho, H.S. Uhm, Chem. Phys. Lett. **427**(4–6), 390 (2006)
15. N.H. Rizvi, Riken Rev. **107** (2003)
16. W. Xiong, Y.S. Zhou, M. Mahjouri-Samani, W.Q. Yang, K.J. Yi, X.N. He, S.H. Liou, Y.F. Lu, Nanotechnology **20**(2), 25601 (2009)
17. K.B.K. Teo, S.B. Lee, M. Chhowalla, V. Semet, V.T. Binh, O. Groening, M. Castignolles, A. Loiseau, G. Pirio, P. Legagneux, Nanotechnology **14**(2), 204 (2003)
18. N.J. Shirtcliffe, G. McHale, M.I. Newton, G. Chabrol, C.C. Perry, Adv. Mater. **16**(21), 1929 (2004)
19. L. Vogelaar, R.G. Lammertink, M. Wessling, Langmuir **22**(7), 3125 (2006)
20. J. Bravo, L. Zhai, Z. Wu, R.E. Cohen, M.F. Rubner, Langmuir **23**(13), 7293 (2007)
21. A. Lafuma, D. Quéré, Nat. Mater. **2**(7), 457 (2003)
22. A.B.D. Cassie, S. Baxter, Trans. Faraday Soc. **40**, 546 (1944)
23. M. Barberoglou, V. Zorba, E. Stratakis, E. Spanakis, P. Tzanetakis, S.H. Anastasiadis, C. Fotakis, Appl. Surf. Sci. **255**(10), 5425 (2009)
24. Z. Wang, C. Lopez, A. Hirsa, N. Koratkar, Appl. Phys. Lett. **91**, 023105 (2007)